Available online at www.sciencedirect.com
ScienceDirect
Trans. Nonferrous Met. Soc. China 32(2022) 3291−3300
Transactions of Nonferrous Metals Society of China
www.tnmsc.cn

Microstructure, phase transformation and mechanical properties of NiMnGa particles/Cu composites fabricated by SPS

Ping GAO[1], Zhao-xin LIU[1,2], Bing TIAN[1], Yun-xiang TONG[1], Feng CHEN[1], Li LI[1]

1. Institute of Materials Processing and Intelligent Manufacturing, College of Materials Science and Chemical Engineering, Harbin Engineering University, Harbin 150001, China;
2. Sunrui Marine Environment Engineering Co., Ltd., Qingdao 266101, China

Received 8 September 2021; accepted 25 March 2022

Abstract: Microstructure, phase transformation and mechanical properties of NiMnGa particles/Cu composites prepared by spark plasma sintering method were investigated by SEM, EDS, XRD, susceptibility measurements and mechanical tests. The NiMnGa particles were found to react with Cu matrix and the composites exhibited a similar crystal structure to the Cu matrix. The martensitic transformation and Curie transition of the composites were weakened due to the composition change of NiMnGa particles caused by reactions. With increasing NiMnGa particles content, the martensitic transformation and Curie transition of the composites were enhanced to some extent. However, the martensitic transformation temperature and Curie transition temperature were decreased by ~50 K as compared to those of the original NiMnGa particles. The compressive strength of the composites increased with the increase of NiMnGa particles content, whereas the compressive strain was decreased gradually.

Key words: NiMnGa alloys; Cu composites; spark plasma sintering; microstructure; phase transformation; mechanical properties

1 Introduction

NiMnGa ferromagnetic shape memory alloys are well known for the large magnetic field induced strain (MFIS) (6%−10%) [1,2], which have been extensively investigated on the martensitic transformation [3−5], magnetic property [6−9] and MFIS [10−12] in the past few years. However, this kind of alloy has a large brittleness and thus exhibits a low workability and mechanical property, which is unfavorable for the practical applications. In order to overcome this problem, a feasible method is to embed NiMnGa particles in a ductile matrix to make composites, in which the matrix provides integrity and good workability and the NiMnGa particles offer functional properties [13,14]. Polymers including polyurethane [15,16], epoxy resin [17,18], and silicone [19] have been selected as matrix to composite with NiMnGa particles. It is found that the composites have exhibited an enhanced damping performance due to the additional energy absorption from NiMnGa particles [15,16,19].

Although it has been mostly used as matrix for the NiMnGa composites, polymer usually exhibits low mechanical strength and the interfacial bonding between polymer and NiMnGa particles is commonly weak, which is unfavorable for the stress transfer upon mechanical loading. In comparison, metals generally have higher mechanical strength and can exhibit better interfacial bonding with NiMnGa alloy by proper chemical reaction. Recently, Mg has been employed as the matrix to

Corresponding author: Bing TIAN, Tel/Fax: +86-451-82518644, E-mail: tianbing@hrbeu.edu.cn
DOI: 10.1016/S1003-6326(22)66020-5

composite with NiMnGa particles [20,21] and the composites exhibit a much higher mechanical strength and ductility as compared to individual Mg or NiMnGa alloy, meanwhile, the composites exhibit a similar martensitic transformation behavior to the original NiMnGa particles. The interfacial reactions between Mg matrix and NiMnGa particles can be adjusted properly by changing NiMnGa particle size. Therefore, the metal could be a potential candidate as matrix to make NiMnGa composites.

Cu has large plasticity, good thermal and electrical conductivity but low mechanical strength and abrasive resistance. In order to enhance mechanical properties of Cu, some hard particles, such as SiC [22,23] and Al_2O_3 [24,25], have been added into Cu to make composites. In consideration of the drawbacks of NiMnGa alloy and Cu, the combination of NiMnGa alloy and Cu could provide a promising way to overcome these problems. Based on the above analysis, the composites composed of NiMnGa and Cu have been raised and investigated in this work. The spark plasma sintering (SPS) technique has been widely used for preparation of metal matrix composites [20,21,26,27] due to its advantages of rapid sintering forming with low sintering temperature, short sintering time and merit of saving energy. Therefore, in the present work, the composites consisting of NiMnGa particles and Cu matrix were fabricated by SPS technique and then the microstructure, phase transformation and mechanical properties of the composites were systematically investigated. The research results could provide an experimental reference for the development of novel NiMnGa composites or Cu composites in the future.

2 Experimental

$Ni_{49.8}Mn_{28.5}Ga_{21.7}$ ferromagnetic shape memory alloy ingot was prepared by arc-melting of high purity elements of Ni, Mn and Ga under argon atmosphere. Then the as-cast ingot was homogenized in vacuum at 1123 K for 12 h followed by water-quenching. The homogenized NiMnGa ingot was crushed and ball milled to fine particles and then annealed at 1073 K for 1 h to recover phase transformation [28]. Commercial Cu powders with spherical shape prepared by atomization method were provided by Chuang Ying Metal Materials Company, China. The annealed NiMnGa powder and the Cu powder were mixed in a steel vial by using QM−3A vibration ball mill (manufactured by Nanjing University Instrument Plant, China) for 30 min without balls. Then, the mixed powder was sintered under a pressure of 40 MPa at 1073 K for 5 min in vacuum using a spark plasma sintering device (SPS−1050). Finally, the NiMnGa/Cu composites with volume fractions of 20%, 30% and 40% NiMnGa particles were obtained, and pure Cu was also fabricated by the same procedure as a control sample.

Microstructure of the composites was characterized using a FEI Apreo-C scanning electron microscope (SEM) equipped with an energy dispersive spectroscopy (EDS) analyzer. Phase constitution was identified by X-ray diffraction (XRD) using a Panalytical X-pert PRO diffractometer with Cu K_α radiation at room temperature. Martensitic transformation and Curie transition were determined by measuring the temperature dependence of low-field ac-magnetic susceptibility using a multi-parameter magnetic measurement system (manufactured by Institute of Physics, Chinese Academy of Sciences). The compression tests were carried out using an Instron universal testing machine (Model 3365) at a deformation speed of 0.5 mm/min. The size of the compression samples was ~d2.5 mm × 4 mm.

3 Results and discussion

3.1 Microstructure of composites

Figures 1(a) and (b) show SEM images of NiMnGa particles and Cu particles, respectively. It can be seen that the NiMnGa particles exhibit an irregular shape with size of <100 μm and the Cu particles mainly exhibit spherical shape with size of <50 μm. Figures 1(c, d, e, f) show backscattered electron SEM images of sintered pure Cu, 20%, 30%, and 40% composites, respectively. It is seen that the pure Cu is very dense and there are almost no sintered holes observed, and it seems to exhibit one single phase with grey color. With the addition of NiMnGa particles, the composites become different from the pure Cu and they are mainly composed of two phases colored in light grey and dark grey, respectively, in which the light grey phase seems to occupy relatively large amount. With

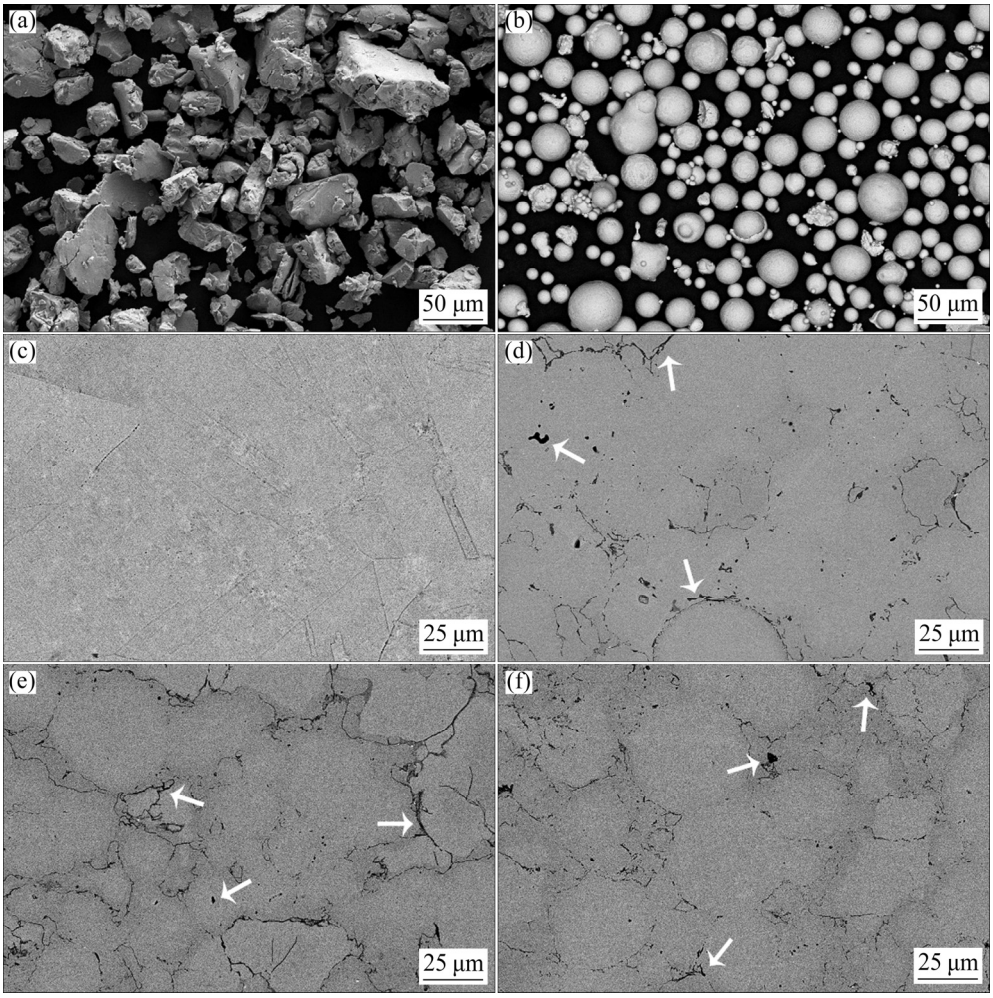

Fig. 1 SEM images of NiMnGa powder (a), Cu powder (b), pure Cu (c), and 20% (d), 30% (e) and 40% (f) NiMnGa/Cu composites

increasing NiMnGa content, the content of dark grey phase seems to be increased. Therefore, it is speculated that the light grey phase should be Cu matrix and the dark grey phase is NiMnGa particle. In addition, it is noted that, as compared to the pure Cu, some small black phases have also been found in the composites, as indicated by arrows in the figures, and it is seen that the black phases exhibit different shapes and randomly distribute in the composites. As compared to the NiMnGa particles/Mg composites [20,21], it is found that NiMnGa and Mg exhibit a strong color contrast and the individual NiMnGa particles can be clearly distinguished. But for the present NiMnGa particles/Cu composites, the contrast between NiMnGa and Cu is weak, which should be caused by that NiMnGa and Cu have a similar molar mass that results in a low contrast in the backscattered electron SEM images.

To further distinguish the NiMnGa particles distribution, the EDS mapping test was performed on all the composites and the EDS mapping results for the 40% NiMnGa composite are shown in Fig. 2. Figure 2(a) shows the SEM image of testing area for 40% NiMnGa composite. The overlay of Cu, Ni, Mn and Ga elemental EDS maps is shown in Fig. 2(b), in which the distribution of NiMnGa particles can be seen. From the color distribution, it seems that some elements have cross-distributed between the Cu matrix and NiMnGa particles. Furthermore, some Mn-rich phases colored in green, as indicated by arrows, have been found, which well corresponds to the black phases shown in Fig. 2(a) which are also indicated by arrows, indicating that partial Mn elements have aggregated in some local areas. Figures 2(c, d, e, f) show individual Cu, Ni, Mn and Ga elemental EDS mapping results, respectively. In Fig. 2(c), it is clearly seen that some Cu elements are distributed in the NiMnGa particles area. For

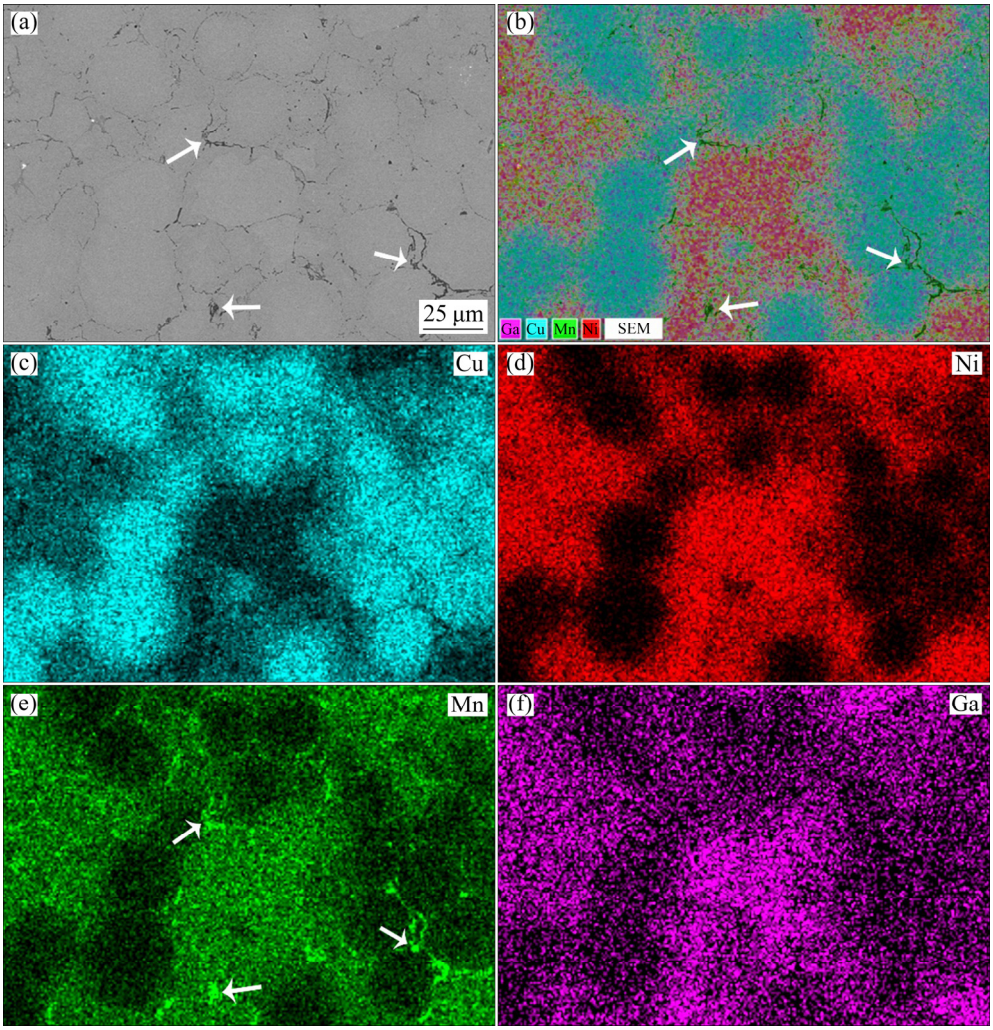

Fig. 2 SEM image of 40%NiMnGa/Cu composite (a) with corresponding EDS maps of overlay (b), Cu (c), Ni (d), Mn (e), and Ga (f)

the Ni element distribution shown in Fig. 2(d), it is noted that most of the Ni elements are distributed in the NiMnGa particles area and there are very few Ni elements distributed in the Cu matrix. However, for the distribution of Mn and Ga elements shown in Figs. 2(e) and (f), respectively, it can be seen that, a large amount of Mn and Ga elements have been found in the Cu matrix area. It is also noted in Fig. 2(e) that the high content of Mn distribution area indicated by arrows is consistent with the areas shown in Figs. 2(a) and (b). This result means that the black phases shown in Fig. 1 are thought to be Mn-rich phases. The similar EDS mapping results have also been obtained in the 20% and 30% NiMnGa composites. These results indicate that the NiMnGa particles have reacted violently with the Cu matrix, which results in the interdiffusion of the elements. This is also different from the NiMnGa/Mg composites [21], in which although the small size NiMnGa particles react severely with Mg matrix, the reaction product only exists in the local interfacial area between the NiMnGa particles and Mg matrix.

From Fig. 2, it can be seen that the circular region mainly corresponds to the Cu matrix, the irregular shape area indicates the NiMnGa particles and the black phase is Mn-rich phase. To further detect the composition of the Cu matrix, NiMnGa particles and Mn-rich phase, the EDS point testing was performed. Figure 3 shows the EDS point testing results of 40%NiMnGa/Cu composite. Figure 3(a) shows the SEM image of the 40% NiMnGa/Cu composites, in which the EDS point testing positions are indicated by arrows for the particle and matrix (Points 1 and 2 are tested on the NiMnGa particle and Cu matrix, respectively). Figure 3(b) shows the enlarged SEM image for EDS point testing of the black Mn-rich phase (Point

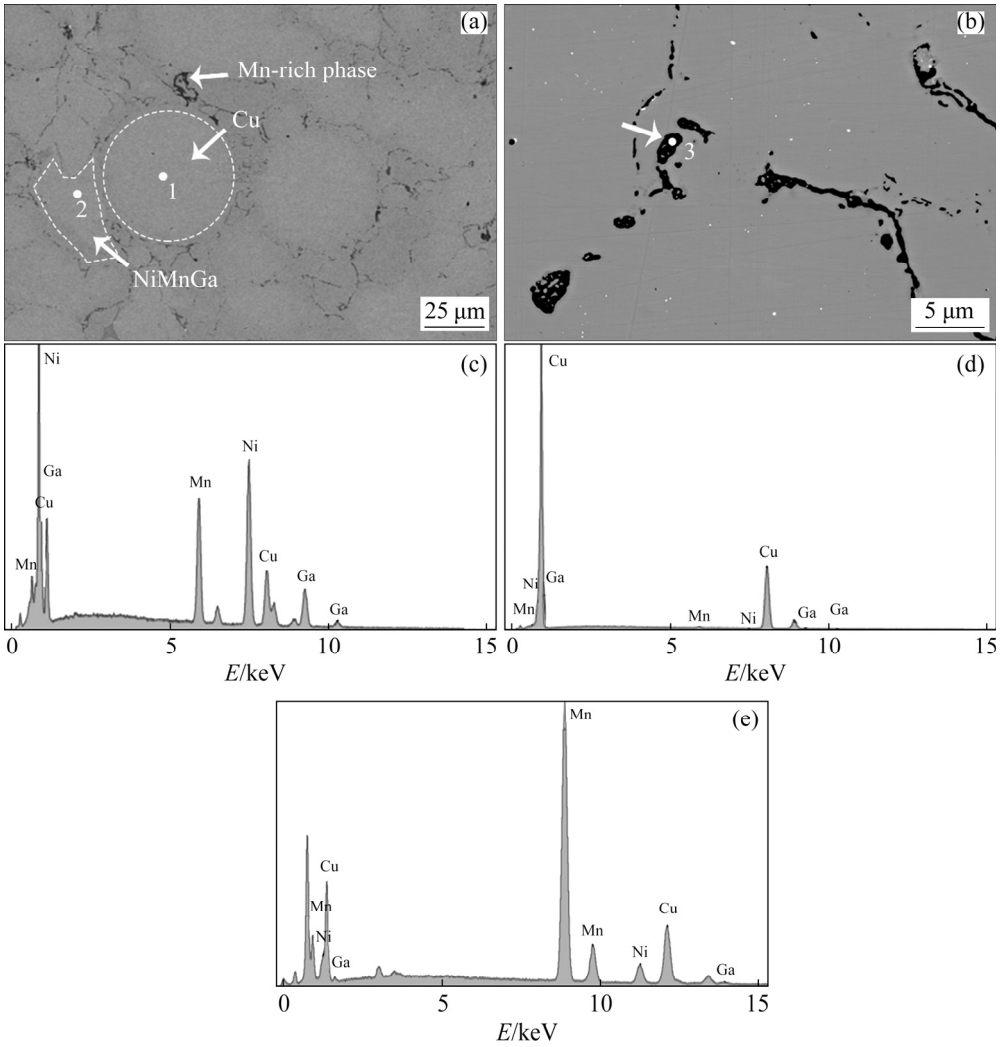

Fig. 3 SEM images (a, b) with high magnification of 40%NiMnGa/Cu composite, and EDS point testing results of Point 1 (c), Point 2 (d) and Point 3 (e)

3 is the testing position). Figures 3(c, d, e) are EDS patterns of Points 1, 2 and 3, respectively, and the corresponding composition derived from the patterns is shown in Table 1. It can be seen from the result in the Point 1 that Cu occupies a relatively large content in the NiMnGa particle. For the result in the Point 2, Ni, Mn and Ga elements can also be found in the Cu matrix, but the content of Ni, Mn and Ga is not high. In the Point 3 for the Mn-rich phase, the Mn element has the largest content, and meanwhile a relatively large amount of Cu and very few Ni and Ga can be found. The point testing results are consistent with the EDS mapping results shown in Fig. 2. This also further confirms that the spherical shape area and the irregular part mainly corresponds to Cu matrix and NiMnGa particles, respectively, and the black phase is a Mn-rich phase containing Cu, Ni and Ga elements.

Table 1 EDS point testing results of 40%NiMnGa/Cu composites (at.%)

Point No.	Ni	Mn	Ga	Cu
1 (NiMnGa particle)	43.16	20.33	19.14	17.37
2 (Cu matrix)	0.24	1.08	0.97	97.71
3 (Mn-rich phase)	7.38	64.82	1.28	26.52

Figure 4 shows XRD patterns of the NiMnGa powder, Cu powder, and NiMnGa/Cu composites. The NiMnGa powder is mainly indexed as a mixture of tetragonal martensite phase and cubic austenite phase [28], and the Cu powder is indexed as face-centered cubic (fcc) structure. It is noted that the diffraction peaks of all the NiMnGa/Cu composites are similar to those of the Cu powder. In 40% NiMnGa composite, only diffraction peak A(220) of austenite phase for the NiMnGa powder

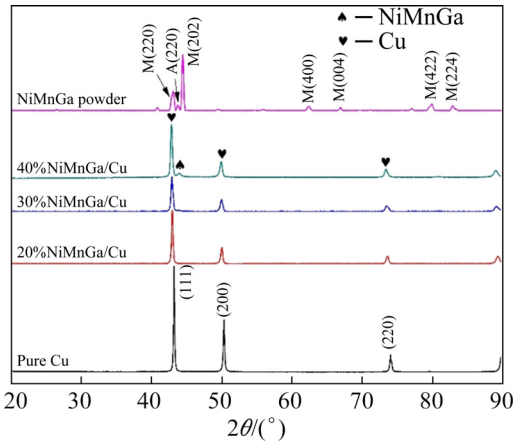

Fig. 4 XRD patterns of NiMnGa powder, Cu powder, and 20%, 30% and 40%NiMnGa/Cu composites

can be found, and the diffraction peaks of martensite phase shown in the original NiMnGa powder are not observed, which should be attributed to the decrease of martensitic transformation temperature for the NiMnGa particles in the composite (it has been verified by the following susceptibility measurement). In 20% and 30% NiMnGa composites, no diffraction peaks belonging to NiMnGa particles are observed. In addition, although the Mn-rich phase has been observed in composites, the diffraction peaks of the Mn-rich phase are not found in the XRD results, which could be caused by low content of the Mn-rich phase.

3.2 Phase transformation of composites

It is further noted that all the diffraction peaks of the composites shift left a little as compared to those of the pure Cu, which should be caused by the introduction of Mn, Ga and Ni elements in the Cu matrix that results in the lattice expansion and increase of interplanar spacing. This indicates that the introduced Ni, Mn and Ga elements have formed solid solution with Cu matrix. It is different from the NiMnGa/Mg composites [21], in which the reaction between NiMnGa particles and Mg matrix are mainly concentrated on the interfacial local area and the new intermetallics rather than solid solution are formed by the interfacial reaction. The disappearance of NiMnGa phase in the 20% and 30% NiMnGa composites should be related to the fact that the initial low content of NiMnGa and the reactions further reduce the content of pure NiMnGa particles. Thus, the low content of pure NiMnGa phase and Mn-rich phase could be beyond detection range of the XRD equipment and results in the disappearance of the diffraction peaks for both phases.

Figure 5 shows the susceptibility−temperature curves of NiMnGa powder and NiMnGa particles/Cu composites. It can be seen that the NiMnGa powder exhibits a remarkable martensitic transformation (A→M, 303−306 K) with susceptibility sudden drop on cooling and austenitic transformation (M→A, 316−320 K) with susceptibility sudden rise on heating, and the Curie transition temperature (from ferromagnetic austenite to paramagnetic austenite) with nearly zero hysteresis is at around 371 K, as shown in Fig. 5(a). The T_M and T_A indicated at the largest slope of the A→M and M→A transformation curves represent martensitic transformation temperature and austenitic transformation temperature, respectively. The T_C indicated at the largest slope of the Curie transition curve stands for Curie temperature. For the 20% NiMnGa composite shown in Fig. 5(b), it is seen that the martensitic transformation and Curie transition cannot be apparently detected. With increasing NiMnGa particles content to 30% shown in Fig. 5(c), we can see that the relatively weak Curie transition at around 310 K has been observed, furthermore a thermal hysteresis at 250−300 K between heating and cooling curves can be seen, indicating the existence of martensitic transformation. This means that some intact NiMnGa particles remain after interactions between NiMnGa and Cu with increasing NiMnGa content, which results in the appearance of martensitic transformation and Curie transition. For the 40% NiMnGa composite (Fig. 5(d)), the Curie transition and martensitic transformation seem to be further enhanced as compared to those of the 30% NiMnGa composite due to the increase of NiMnGa particles content. These results are consistent with the XRD results shown in Fig. 4, in which the diffraction peak belonging to NiMnGa particles has been observed in the 40% NiMnGa composite.

In addition, it is found that the Curie temperature and martensitic transformation temperature of the composites have been apparently reduced as compared to that of the original NiMnGa particles. It is much different from the NiMnGa/Mg composite [21], in which although the

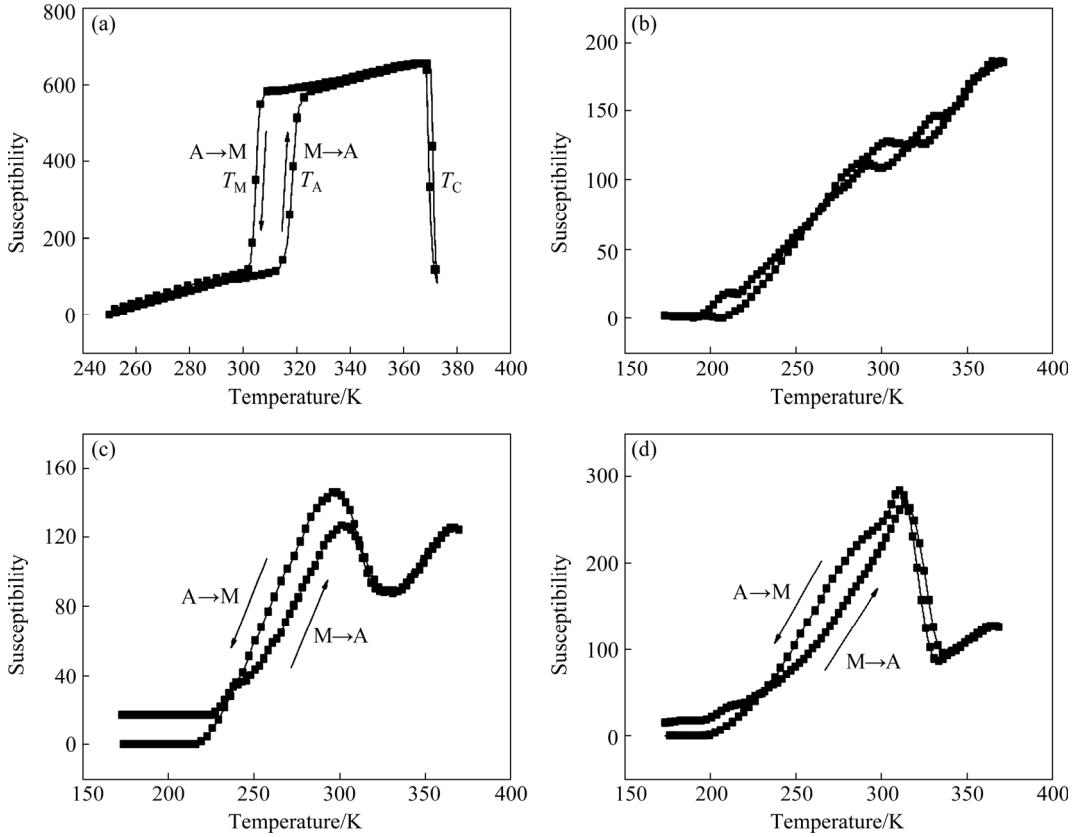

Fig. 5 Susceptibility−temperature curves of NiMnGa powder (a), and 20% (b), 30% (c) and 40% (d) NiMnGa/Cu composites

NiMnGa particles have severe interfacial reactions with the Mg matrix, but the Curie transition and martensitic transformation temperatures are still similar to those of the original particles, and the reaction mainly occurs in the interfacial area and there are no elemental diffusions with long distance. In the present NiMnGa/Cu composites, the reactions have resulted in the elemental interdiffusion between the NiMnGa particles and Cu matrix, and meanwhile, the aggregation of Mn elements during diffusion process occurs in some local areas. This indicates that the reaction mechanism between NiMnGa particles with Mg matrix and with Cu matrix are different, which results in the different properties of the composites. It is noted that, for the Cu composite, the sintering temperature is 1073 K and the pressure is 40 MPa, which are much higher than those for the preparation of NiMnGa/Mg composites (the sintering temperature is 773 K and the pressure is 20 MPa). Therefore, the much higher sintering temperature and pressure in the NiMnGa/Cu composites should have provided higher diffusion driving force for the elemental diffusions than those for the NiMnGa/Mg composites, which should be the main reason for the different reaction phenomena obtained in both composites.

3.3 Mechanical properties of composites

Figure 6 shows the compressive stress−strain curves of pure Cu and NiMnGa particles/Cu composites. It is found that the pure Cu does not fracture during compression (it is compressed to a thin sheet ultimately) and the partial compressive curve of the pure Cu is given in the figure. After the addition of NiMnGa particles, it can be seen from the curves that the composites can be fractured during the compression, indicating the reduction of ductility due to the addition of NiMnGa particles. However, the mechanical strength of the composites is greatly enhanced after the addition of NiMnGa particles. The compressive strength is increased gradually with increasing NiMnGa particles, but the compressive strain is reduced gradually. The compressive strength and ductility of the 40% NiMnGa composite reach up to 865 MPa and 30%, respectively, which are higher than those of the Cu−Al_2O_3 nanocomposites [24].

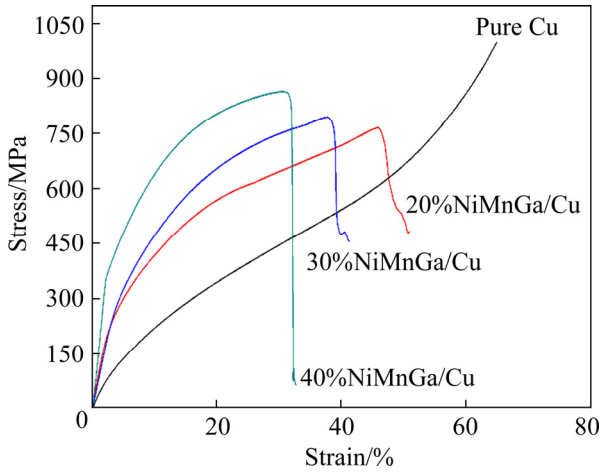

Fig. 6 Compressive stress–strain curves of pure Cu, 20%, 30%, and 40%NiMnGa/Cu composites

The fracture surfaces of the NiMnGa particles/Cu composites are shown in Fig. 7. Figures 7(a, c, e) show the low magnification SEM images of 20%, 30% and 40% NiMnGa composites, respectively. It can be seen that the fracture surfaces of the three samples are similar and some small holes and cracks can be seen on the surface, as indicated by arrows in the figure. The holes could come from the sintering process or from the split of small Mn-rich phases. It is noted that there is no apparent individual NiMnGa particles observed in the figure. Figures 7(b, d, f) show the fracture surfaces with high magnification of 20%, 30% and 40% NiMnGa composites, respectively. These figures are mainly selected on the cracks part shown in the low magnification images. For 20% NiMnGa composite, many dimples can be seen on the surface as indicated by arrows, which indicates a good ductility of the composite. With increasing NiMnGa content to 30% and 40%, we can see that the dimples can also be seen on the surface, but the quantity and size of the dimples seem to be reduced gradually, as indicated by arrows. The reduction of dimple size and quantity indicates the reduction of ductility of the composites. It is suggested that the introduction of Mn, Ga or Ni elements into the Cu matrix has resulted in the solution strengthening

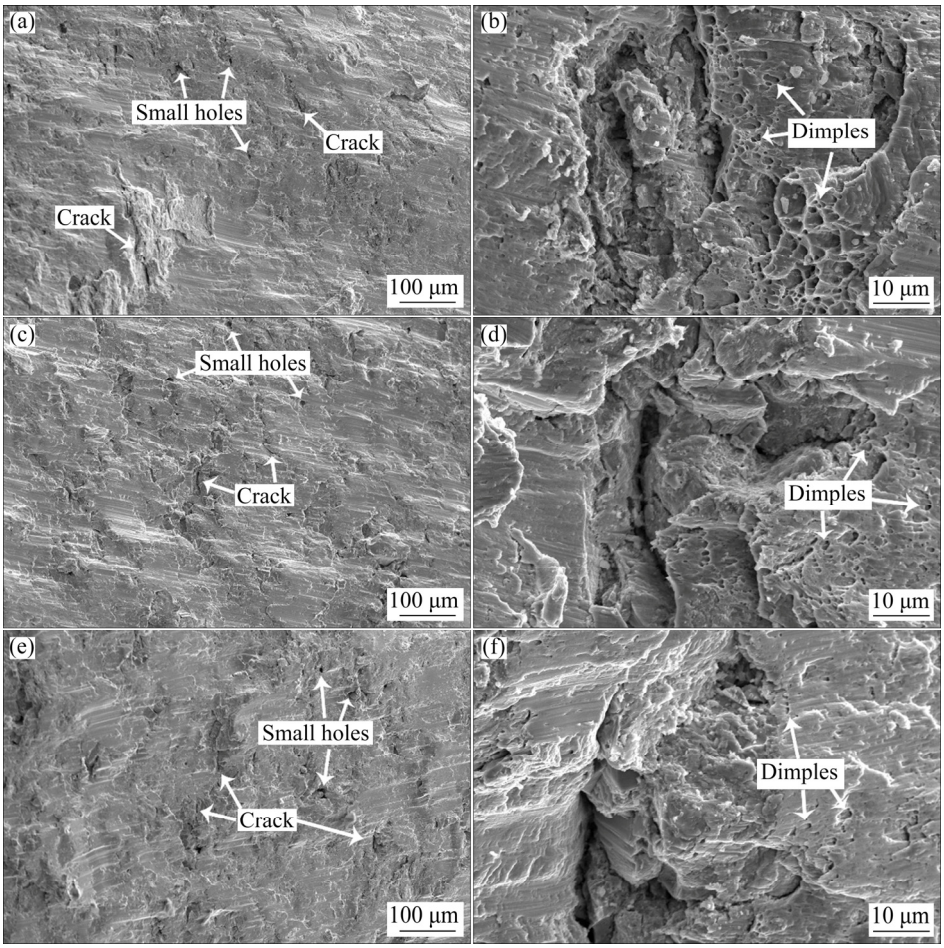

Fig. 7 Fracture surfaces of 20% (a, b), 30% (c, d), and 40% (e, f) NiMnGa/Cu composites

effect, and meanwhile, the remained NiMnGa particles and formed Mn-rich phases also enhance the mechanical strength by particle reinforcing effect. Therefore, the enhancement of mechanical strength of the Cu matrix should be related to the two factors: solution strengthening and particles strengthening. Whereas, the irregular Mn-rich phases acting as a brittle matter could form a weak interfacial bonding with the Cu matrix, therefore, the existence of Mn-rich phases and some sintered holes could be favorable for the origins of cracks and propagation of cracks, thus reducing the ductility of the composites.

4 Conclusions

(1) The NiMnGa particles react with the Cu matrix during sintering, which results in the interdiffusion of Mn, Ga and Ni elements with the Cu element and formation of Mn-rich phases.

(2) For the 20% NiMnGa composite, the martensitic transformation and Curie transition nearly disappear. With increasing NiMnGa content to 30% and 40%, the martensitic transformation of the composites is enhanced and occurs. The martensitic transformation temperature and Curie temperature of the composites are reduced, as compared to those of the original NiMnGa particles.

(3) The enhancement of compressive strength of the composites with the addition of NiMnGa particles and with the increase of NiMnGa content should be related to the two factors: solution strengthening and particles reinforcement. The reduction of ductility as compared to the pure Cu should be caused by the existence of brittle Mn-rich phases and sintered defects that result in the crack formation and propagation.

Acknowledgments

This study was supported by the National Natural Science Foundation of China (No. 51201044), High-level Scientific Research Guidance Project of Harbin Engineering University, China (No. 3072022TS1006), Postdoctoral Scientific Research Developmental Fund of Heilongjiang Province, China (No. LBH-Q16046), and Key Laboratory of Superlight Materials & Surface Technology (Harbin Engineering University), Ministry of Education, China.

References

[1] SOZINOV A, LIKHACHEV A A, LANSKA N, ULLAKKO K. Giant magnetic-field-induced strain in NiMnGa seven-layered martensitic phase [J]. Applied Physics Letters, 2002, 80(10): 1746−1748.

[2] JIANG Cheng-bao, WANG Jing-min, XU Hui-bin. Temperature dependence of the giant magnetostrain in a NiMnGa magnetic shape memory alloy [J]. Applied Physics Letters, 2005, 86(25): 252508.

[3] MA Yun-qing, JIANG Cheng-bao, LI Yan, XU Hui-bin, WANG Cui-ping, LIU Xing-jun. Study of $Ni_{50+x}Mn_{25}$-Ga_{25-x} (x=2−11) as high-temperature shape-memory alloys [J]. Acta Materialia, 2007, 55(5): 1533−1541.

[4] TAN Chang-long, FENG Zhi-cheng, ZHANG Kun, WU Ming-yang, TIAN Xiao-hua, GUO Er-jun. Microstructure, martensitic transformation and mechanical properties of Ni−Mn−Sn alloys by substituting Fe for Ni [J]. Transactions of Nonferrous Metals Society of China, 2017, 27: 2234−2238.

[5] WANG Jun-song, TIAN Bing, TONG Yun-xiang, CHEN Feng, LI Li. Effect of thermal treatment and ball milling on microstructure and phase transformation of Ni−Mn−Ga−Nb alloys [J]. Transactions of Nonferrous Metals Society of China, 2019, 29(10): 2117−2127.

[6] WANG Jing-min, JIANG Cheng-bao, TECHAPIESAN-CHAROENKIJ R, BONO D, ALLEN S M, O′HANDLEY R C. Microstructure and magnetic properties of melt spinning Ni−Mn−Ga [J]. Intermetallics, 2013, 32: 151−155.

[7] ZHENG P Q, KUCZA N J, PATRICK C L, MÜLLNER P, DUNAND D C. Mechanical and magnetic behavior of oligocrystalline Ni−Mn−Ga microwires [J]. Journal of Alloys and Compounds, 2015, 624: 226−233.

[8] BAI Jing, LI Ze, WAN Zhen, ZHAO Xiang. A first-principles study on crystal structure, phase stability and magnetic properties of Ni−Mn−Ga−Cu ferromagnetic shape memory alloys [J]. Acta Metallurgica Sinica, 2017, 53(1): 83−89.

[9] TIAN X H, SUI J H, ZHANG X, ZHENG X H, CAI W. Grain size effect on martensitic transformation, mechanical and magnetic properties of Ni−Mn−Ga alloy fabricated by spark plasma sintering [J]. Journal of Alloys and Compounds, 2012, 514: 210−213.

[10] ZHAO Zeng-qi, WU Shuang-xia, WANG Fang-shu, WANG Qiang, JIANG Li-ping, WANG Xin-lin. Large magnetic-field-induced strains in rare earth polycrystalline Ni−Mn−Ga [J]. Rare Metals, 2004, 23(3): 241−245.

[11] CHMIELUS M, ZHANG X X, WITHERSPOON C, DUNAND D C, MÜLLNER P. Giant magnetic-field-induced strains in polycrystalline Ni−Mn−Ga foams [J]. Nature Materials, 2009, 8(11): 863−866.

[12] LI Zhen-zhuang, LI Zong-bin, YANG Bo, HE Xi-jia, GAN Wei-min, ZHANG Yuan-lei, LI Zhe, ZHANG Yu-dong, ESLING C, ZHAO Xiang, ZUO Liang. Over 2% magnetic-field-induced strain in a polycrystalline $Ni_{50}Mn_{28.5}$-$Ga_{21.5}$ alloy prepared by directional solidification [J]. Materials Science and Engineering A, 2020, 780: 139170.

[13] LIU J, SCHEERBAUM N, KAUFFMANN-WEISS S, GUTFLEISCH O. NiMn-based alloys and composites for magnetically controlled dampers and actuators [J]. Advanced Engineering Materials, 2012, 14(8): 653−667.
[14] HOSODA H, TAKEUCHI S, INAMURA T, WAKASHIMA K. Material design and shape memory properties of smart composites composed of polymer and ferromagnetic shape memory alloy particles [J]. Science and Technology of Advanced Materials, 2004, 5(4): 503−509.
[15] FEUCHTWANGER J, MICHAEL S, JUANG J K, BONO D, O'HANDLEY R C, ALLEN S M, JENKINS C, GOLDIE J, BERKOWITZ A. Energy absorption in Ni–Mn–Ga polymer composites [J]. Journal of Applied Physics, 2003, 93(10): 8528−8530.
[16] FEUCHTWANGER J, RICHARD M L, TANG Y J, BERKOWITZ A E, O'HANDLEY R C, ALLEN S M. Large energy absorption in Ni–Mn–Ga/polymer composites [J]. Journal of Applied Physics, 2005, 97(10): 10M319.
[17] SCHEERBAUM N, HINZ D, GUTFLEISCH O, MÜLLER K H, SCHULTZ L. Textured polymer bonded composites with Ni–Mn–Ga magnetic shape memory particles [J]. Acta Materialia, 2007, 55(8): 2707−2713.
[18] TIAN B, CHEN F, TONG Y X, LI L, ZHENG Y F. Bending properties of epoxy resin matrix composites filled with Ni–Mn–Ga ferromagnetic shape memory alloy powders [J]. Materials Letters, 2009, 63(20): 1729−1732.
[19] FEUCHTWANGER J, SEIF E, SRATONGON P, HOSODA H, CHERNENKO V A. Vibration damping of Ni−Mn−Ga/silicone composites [J]. Scripta Materialia, 2018, 146: 9−12.
[20] TIAN B, TONG Y X, CHEN F, LI L, ZHENG Y F. Microstructure, phase transformation and mechanical property of Ni–Mn–Ga particles/Mg composites [J]. Materials Science and Engineering A, 2014, 615: 273−277.
[21] TIAN B, CHENG Z G, TONG Y X, LI L, ZHENG Y F, LI Q Z. Effect of enhanced interfacial reaction on the microstructure, phase transformation and mechanical property of Ni–Mn–Ga particles/Mg composites [J]. Materials & Design, 2015, 82: 77−83.
[22] CHEN Guo-qin, XIU Zi-yang, MENG Song-he, WU Gao-hui, ZHU De-zhi. Thermal expansion and mechanical properties of high reinforcement content SiC_p/Cu composites fabricated by squeeze casting technology [J]. Transactions of Nonferrous Metals Society of China, 2009, 19(S3): s600−s604.
[23] BARMOUZ M, ASADI P, BESHARATI GIVI M K, TAHERISHARGH M. Investigation of mechanical properties of Cu/SiC composite fabricated by FSP: Effect of SiC particles' size and volume fraction [J]. Materials Science and Engineering A, 2011, 528(3): 1740−1749.
[24] TIAN Bao-hong, LIU Ping, SONG Ke-xing, LI Yan, LIU Yong, REN Feng-zhang, SU Juan-hua. Microstructure and properties at elevated temperature of a nano-Al_2O_3 particles dispersion-strengthened copper base composite [J]. Materials Science and Engineering A, 2006, 435/436: 705−710.
[25] LIU Xiang-bing, JIA Cheng-chang, CHEN Xiao-hua, GAI Guo-sheng. Microstructures and properties of 1.0%Al_2O_3/Cu composite treated by rolling [J]. Transactions of Nonferrous Metals Society of China, 2007, 17(S1): s626−s629.
[26] HONG Yu, WANG Wu-jie, LIU Jia-qin, TANG Wen-ming, WU Yu-cheng. Effect of porosity and interface structures on thermal and mechanical properties of SiC_p/6061Al composites with high volume fraction of SiC [J]. Transactions of Nonferrous Metals Society of China, 2019, 29(5): 941−949.
[27] NIE Qiang-qiang, CHEN Guo-hong, WANG Bing, YANG Lei, TANG Wen-ming. Process optimization, microstructures and mechanical/thermal properties of Cu/Invar bi-metal matrix composites fabricated by spark plasma sintering [J]. Transactions of Nonferrous Metals Society of China, 2021, 31(10): 3050−3062.
[28] TIAN B, CHEN F, LIU Y, ZHENG Y F. Structural transition and atomic ordering of $Ni_{49.8}Mn_{28.5}Ga_{21.7}$ ferromagnetic shape memory alloy powders prepared by ball milling [J]. Materials Letters, 2008, 62(17/18): 2851−2854.

SPS 制备 NiMnGa/Cu 复合材料的显微组织、相变和力学性能

高 萍[1]，刘朝信[1,2]，田 兵[1]，佟运祥[1]，陈 枫[1]，李 莉[1]

1. 哈尔滨工程大学 材料科学与化学工程学院 材料加工及智能制造研究所，哈尔滨 150001；
2. 青岛双瑞海洋环境工程股份有限公司，青岛 266101

摘 要：采用 SEM、EDS、XRD、交流磁化率测试和力学测试研究放电等离子体烧结法制备 NiMnGa 颗粒/Cu 复合材料的显微组织、相变和力学性能。研究发现，NiMnGa 颗粒与 Cu 基体发生反应，复合材料具有与 Cu 基体相似的晶体结构。由于反应导致 NiMnGa 颗粒发生成分变化，因此，复合材料的马氏体相变和居里转变被弱化。随着 NiMnGa 颗粒含量增加，复合材料的马氏体相变和居里相变在一定程度上得到增强。与原始 NiMnGa 颗粒相比，复合材料的马氏体相变温度和居里转变温度降低约 50 K。随着 NiMnGa 颗粒含量增加，复合材料的压缩强度得到提高，但压缩应变逐渐降低。

关键词：NiMnGa 合金；Cu 复合材料；放电等离子体烧结；显微组织；相变；力学性能

(Edited by Xiang-qun LI)